GeoScienceWorld
Lithosphere
Volume 2022, Article ID 1699273, 12 pages
https://doi.org/10.2113/2022/1699273

Lithosphere

Research Article

Quantitative Threshold of Energy Fractal Dimension for Immediate Rock Burst Warning in Deep Tunnel: A Case Study

Yang Yu,[1] Guang-liang Feng,[2,3] Chang-jie Xu,[1] Bing-rui Chen,[2] Da-xin Geng,[1] and Bi-tang Zhu[1]

[1]*Key Laboratory of Geotechnical Engineering Infrastructure and Safety Control, East China Jiaotong University, Nanchang 330013, China*
[2]*State Key Laboratory of Geomechanics and Geotechnical Engineering, Institute of Rock and Soil Mechanics, Chinese Academy of Sciences, Wuhan 430071, China*
[3]*Guangxi Key Laboratory of Disaster Prevention and Engineering Safety, Guangxi University, Nanning 530000, China*

Correspondence should be addressed to Guang-liang Feng; glfeng@whrsm.ac.cn

Received 29 November 2021; Accepted 18 January 2022; Published 12 February 2022

Academic Editor: Yonghui Wu

Rock bursts are a serious geological disaster occurring in deep underground engineering operations, which will cause casualties and economic loss. The quantitative threshold of energy fractal dimension for immediate rock burst warning in a deep tunnel was studied. The study was conducted based on the immediate rock burst cases in the deep tunnels of Jinping Hydropower Station, China. Firstly, a fractal dimension calculation method was proposed for deep linear tunnels associated with microseismic monitoring to explore the energy fractal dimension during the 37 immediate rock bursts and their development to events of different intensities (intense and moderate events). On this basis, a mechanism analysis was undertaken to assess the distribution range and evolution of the energy fractal dimension in the development of the immediate rock bursts. Then, the energy fractal dimension, as a quantitative threshold, was taken as a criterion for judging the rock burst risk. Furthermore, the corresponding warning index and dynamic control method were established. This index and method were applied in the subsequent construction process. The results can be used as a guide to establish a dynamic warning system based on the microseismicity monitored and provide a scientific basis for the prediction, warning, and risk-control standard of rock burst disasters during excavation of deep tunnels.

1. Introduction

Rock bursts are a kind of disaster causing the bursting and ejection of rock due to the abrupt release of elastic strain potential energy under high stress from the surrounding rock. They are generally triggered by construction and frequently occur in the construction of deep underground projects [1–4]. Rock bursts are also a worldwide challenge in the field of rock mechanics, for their randomness and abruptness of occurrence. The occurrence of rock burst disasters in the excavation of deep rock tunnels under high stress may cause casualties among workers, damage to devices and equipment, leading to construction delays, and significant economic loss [2, 5–7]. Therefore, the prediction, warning, and control of rock bursts are of significance for the smooth construction of deep underground projects. Rock bursts are divided into immediate rock bursts and time-delayed rock bursts: different types of rock bursts are governed by different underlying mechanisms of behavior [2]. Immediate rock bursts refer to those happening within the range of influence of the excavation unloading effect. Spatially they mainly occur in the tunnel face and the surrounding rock, while temporally they occur between a few hours to several days after excavation. More than 80% of the rock bursts that happened in the construction of deep rock tunnels are immediate rock bursts [8, 9].

With the constant development of construction of tunnel projects, the characteristics of underground tunnels including large burial depth, long tunnel lines, large tunnel diameters, and presence of tunnel groups become increasingly

apparent. In addition, the risk of rock bursts also becomes more prominent, which, in turn, also promotes research into rock bursts. Differing from rocks involved in shallow underground projects, which are subordinated to a linear mechanical system, rocks in deep engineering projects are treated as a nonlinear mechanical system, thus a part of and even a majority of, the conventional theories, methods, and technologies are inapplicable [8, 10–12]. Microseismic monitoring has been applied to deep underground engineering operations. Durrheim et al. [13] studied rock burst disasters in deep mines by using microseismic monitoring. Researchers have investigated microseismic activities, as precursors to rock bursts, based on the evolution of source parameters of microseismic events before the occurrence of a rock burst. Tang & Xia [14] found that the rock mass in the zone with concentrated microseismic activities before occurrence of rock bursts has increasing stiffness, and the decrease of the stiffness suggests a declining probability of a rock burst. Rock burst cases in Dongguashan copper mine (Tongling City, Anhui Province, China) also provided support for this point of view. Feng et al. [2, 15] established a microseismic method for dynamic warning of rock burst in deep tunnels and ascertained the precursory characteristics of different types and intensities of rock bursts. The research results of Yu et al. [16] implied that the amount of microseismic signals in the rock burst zone constantly increases and the energy parameter rapidly grows as microfractures appear, develop, and converge in the development of a rock burst event.

Acquisition and analysis of the microseismicity, as a precursor to a rock burst, form the basis for developing a warning method for rock bursts based on microseismic monitoring. Fractal theory provides the means with which to assess complex structures and allows researchers to find order in disordered systems [17]. The theory quantifies the self-similarity, irregularity, and degree of crushing of a fractal structure using its fractal dimension. Xie & Pariseau [18] were the first to apply fractal theory to the development of rock burst disasters in mining activities. They pointed out that the lower the spatial fractal dimension of microfracturing events is, the higher the probability of occurrence of rock bursts. Feng et al. [19] found that microfracturing events that occur in the evolution of rock burst disasters in tunnels excavated in a deep rock mass also have a fractal structure. They also evaluated the energy fractal dimension of microseismic events happening in the development and occurrence of different types of rock bursts. Yu et al. [16] indicated that the microseismic location information in the development of rock burst disasters shows a self-similar temporal distribution. Moreover, the more intense the rock burst disaster, the larger the temporal fractal dimension. In addition, the self-similarity from the Gutenberg–Richter relationship showed that there are self-similarity and fractal behaviors in frequency, energy, and magnitude which was obvious across different various fracture scales from large earthquakes to microcracks [16, 20, 21], and there is a fractal characteristic of microseismic events, not only in their worldwide scale but also at a local or regional level [22–24]; however, the quantitative threshold of fractal dimension for immediate rock burst warning in deep tunnel remains unclear.

In the present work, the immediate rock burst cases in the deep tunnels of Jinping Hydropower Station, China, were used. The energy fractal behavior of microseismic events in the development and occurrence of immediate rock bursts was studied by introducing the fractal calculation method. On this basis, a mechanism analysis was conducted on the distribution and evolution of energy fractal dimension. Then, a warning index based on energy fractal dimension with a quantitative threshold for immediate rock burst disasters in deep tunnel was established. The application of this index in the construction process can inhibit the occurrence of rock burst disasters. The research results provide the basis for the prediction, warning, and control of rock burst risk in the excavation of deep tunnels.

2. Project Introduction and Rock Burst Disaster

2.1. Brief Introduction to the Project. The cases studied in the present work come from the deep tunnels of Jinping Hydropower Station, which is located on the Yalong River in Sichuan Province of southwest China. Jinping Hydropower Station uses the natural drop of more than 280 m to cut off the Yalong River. It is considered the backbone of the Yalong River works in terms of its stepped excavation with the highest water head and the largest installed capacity: the installed capacity of the hydropower station is 24,800 MW, and the unit capacity is 600 MW. The project hub is mainly composed of the first gate, the water diversion system, and the tail underground powerhouse (Figure 1).

The geological cross-section of the deep tunnels in Jinping Hydropower Station is shown in Figure 2. In Figure 2, T_1 denotes chlorite schist, T_{2b} is marble of the Baishan formation, T_{2y} represents marble of the Yantang formation, T_{2z} is marble of the Zagunao formation, and T_3 is sandstone and slate. Figure 2 indicates that the maximum burial depth of tunnels (including headrace and water drainage tunnels) is over 2,500 m. The tunnels are mainly formed in type II and III Baishan marble. The physicomechanical indices of the rocks are listed in Table 1.

2.2. Rock Burst Occurrence in the Deep Tunnels. During the construction of the deep tunnels in Jinping Hydropower Station, hundreds of rock bursts occurred with different spatial scales, which affected the safety and schedule of the construction works. Slight rock bursts were the main type that happens in sections accounting for 11.6% of the total length of the tunnel; the proportion of moderate rock bursts was 4.5%, and the occurrence of intense rock bursts was only 1.6%. The main phenomena of rock bursts with different intensities were described in detail elsewhere [25]. The cumulative length of sections affected by rock bursts of various grades was greater than 8 km during excavation of the tunnel. The work undertaken on the deep tunnels in Jinping Hydropower Station shows that the impact of slight rock bursts is small: on this basis, the present research focuses on intense and moderate rock bursts.

Based on the integrated seismic monitoring system from South Africa, the continuous real-time microseismic monitoring was conducted in the four headrace tunnels

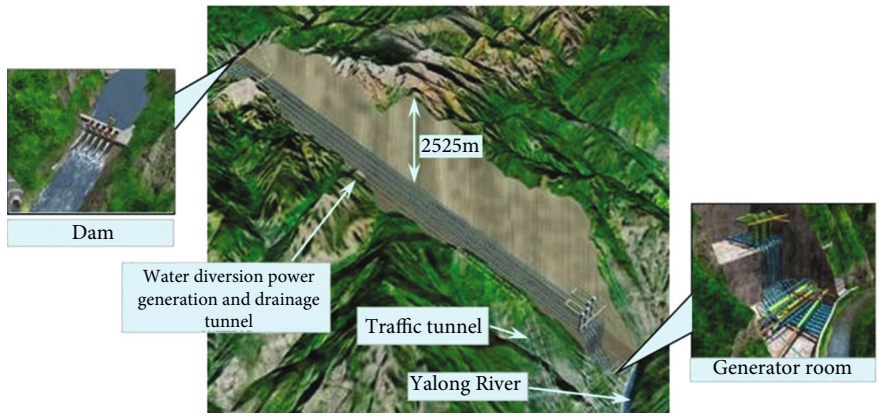

Figure 1: The project hub of Jinping Hydropower Station [7].

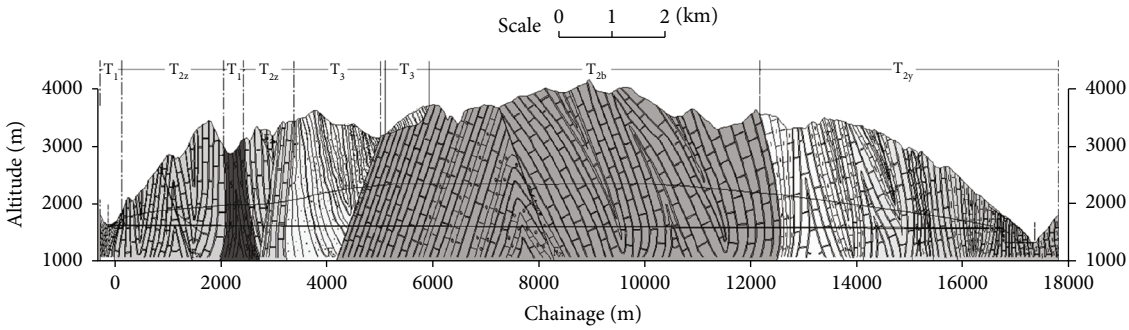

Figure 2: Geological cross-section through Jinping Hydropower Station.

Table 1: Physicomechanical indices for Jinping Baishan marble [25].

Parameter	Value
Bulk weight (kN/m^3)	2.5~2.8 × 10^2
Poisson's ratio	0.21~0.33
Uniaxial compressive strength of saturated rock (MPa)	100~114
Maximum principal stress (MPa)	46~73
Modulus of deformation (GPa)	8~16
Elastic modulus (GPa)	25~40

(diameter, 13 m) and a water drainage tunnel (diameter, 6.5 m) in the Jinping Hydropower Station. The cross-sections of the 1# and 3# headrace tunnels and the water drainage tunnel are circular, and those of 2# and 4# headrace tunnels are horseshoe shaped (Figure 3). The MS monitoring was described elsewhere [25].

3. Fractal Dimension Calculation Based on Characteristics of Microseismic Energy Self-Similar Distribution

3.1. Energy Release Associated with Microseismic Events. There are many cracks generated during the excavation of deep tunnels: during failure, rock masses radiate energy in the form of a stress wave (including *P*-wave and *S*-wave) for each microseismic event. The microseismic energy released, which is caused by elastic deformation becoming inelastic, is one of the most important parameters affecting a rock burst. The energy released from the microseismic source can be received by the installed microseismic monitoring instruments. The energy released is calculated as follows [26]:

$$E_{P,S} = E_P + E_s, \tag{1}$$

where $E_{P,S}$ is the energy released from the microseismic event and E_P and E_s denote the energy released in the form of *P*-wave and *S*-wave, respectively:

$$\begin{aligned} E_P &= \frac{8}{5}\pi\rho v_P R^2 \int_0^{t_S} u^2{}_{\text{corr}}(t)\mathrm{d}t, \\ E_S &= \frac{8}{5}\pi\rho v_S R^2 \int_0^{t_S} u^2{}_{\text{corr}}(t)\mathrm{d}t, \end{aligned} \tag{2}$$

where p denotes the density of the surrounding rock, v_P (v_s) is *P*-wave (*S*-wave) velocity of the rock-mass after excavation, R is the epicentral distance, t_s represents the duration, and $u^2{}_{\text{corr}}(t)$ is the time function of the wave velocity.

3.2. Calculation of Microseismic Energy Fractal Dimension Associated with Immediate Rock Bursts. Feng et al. [2] selected the microseismic events that occurred 10 m in front

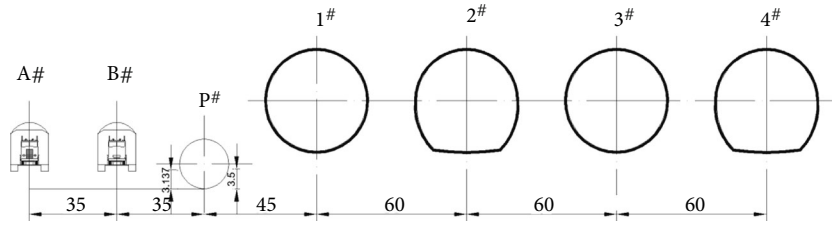

Figure 3: The deep tunnels of Jinping Hydropower Station (all dimensions: m).

and 30 m behind the working face for warning of immediate rock bursts. This range was used for energy fractal investigation of immediate rock bursts. The calculation method of microseismic energy fractal dimension associated with immediate rock bursts was as follows: all microseismic events in the warning zone (10 m in front and 30 m behind the working face) associated with the immediate rock bursts are considered, as shown in Figure 4. In Figure 4, the total number of microseismic event pairs whose energy range $e = \lg E_{P,S} \le E_{\max}$ can then be counted and denoted as $N(e)$:

$$N(e)\ (e \le E_{\max}) = [\text{number of microseismic event pairs within the energy zone } e], \tag{3}$$

where N is the number of the total microseismic events in energy zone $E_{\max}$ and the correlation integral $c(e)$ for the microseismic energy distributions during the rock bursts is expressed in the following form [27]:

$$c(e) = \frac{2N(e)}{N(N-1)}\ (e \le E_{\max}). \tag{4}$$

If the $\lg e - \lg c(e)$ plot is linear, the slope D_e of the best-fit line is the energy fractal dimension of the microseismic events:

$$D_e = \lim_{e \longrightarrow E} \frac{\lg c(e)}{\lg (e)}. \tag{5}$$

Using the calculation method above, fractal dimension of microseismic energy associated with rock bursts was determined at any time, according to the information from the energy distribution of microseismic events.

4. Dynamic Warning Index for Immediate Rock Burst Disasters Based on Fractal Dimension of Microseismic Energy

4.1. Classification of Immediate Rock Bursts. Monitoring data from the Mine-By test tunnel in Canada indicate that under high-stress conditions the stress disturbance mainly occurs between $0.5d$ ahead of and $2d$ behind the working face of diameter d. Meanwhile, the deep headrace tunnels of Jinping II hydropower station show that the stress disturbance mainly occurs between $0.6d$ ahead of and $2d$ diameter behind the working face, with $d = 13$ m. Therefore, stress disturbance mainly occurs between 7.8 m ahead of and 26 m behind the working face during the excavation of deep headrace tunnels of Jinping hydropower station.

Based on the construction progress of 1~4# headrace tunnels (14 months, from October 2010 to December 2011), the average excavation speed was 4.5 m per day. Disturbance mainly occurred between two days ahead of and six days behind, the working face in deep headrace tunnels of Jinping II hydropower station. To ensure the immediate rock burst zone is within the zone of stress disturbance of the working face excavation, an immediate rock burst zone is defined as the zone located between the present working face and its position six days ago, and the time-delay rock burst zone is defined as the zone located beyond the range of the immediate rock burst zone (Figure 5).

4.2. Energy Fractal Behavior Analysis of Typical Rock Burst. At approximately 9:00 a.m. on April 20, 2011, with a loud blast-like sound, a rock burst occurred in the 3# headrace tunnel in Jinping hydropower station, from chainage K6+101 to K6+111. The centerline of the rock burst-pit (chainage K6+105.5) was about 8.5 m behind the working face (chainage K6+114). The rock burst-pit was approximately 8.7 m high and 13 m wide and had a maximum depth of 1.5 m. The surrounding rock was thick with coarse grains and no surface plane. According to its time and area of occurrence, the rock burst on April 20, 2011, was classified as an immediate intense rock burst. The spatial and energy distributions of microseismic events during its evolution are shown in Figure 6, whose minimum and maximum energies (in logarithmic) of microseismic events were 0.53 and 6.56, respectively.

Microseismic events in the zone 10 m ahead of and 30 m behind the present working face were selected for energy fractal calculation. The time range is 24 h, in increments of 4 h ($t = 0, 4, 8, 12, \cdots, 24$) before the occurrence of the rock burst. According to the energy fractal calculation method used for analysis of microseismic events (Section 3.2), and based on the energy distribution of microseismic events (Figure 6), the values of N and $N(e)$ were obtained, and the values of $\lg e$ and $\lg c(e)$ were calculated. Linear fitting gave $\lg c(s)$ as the y -coordinate (Equation (4)) and energy range $\lg e$ as the x -coordinate (here: 2, 3, 4, 5, and the maximum spatial range $\lg E = 6.56$): Figures 7(a) and 7(b) show the energy fractal fitting chart and the evolution of energy fractal dimension for 24 h before the immediate intense rock burst on April 20, 2011. The time range of energy fractal

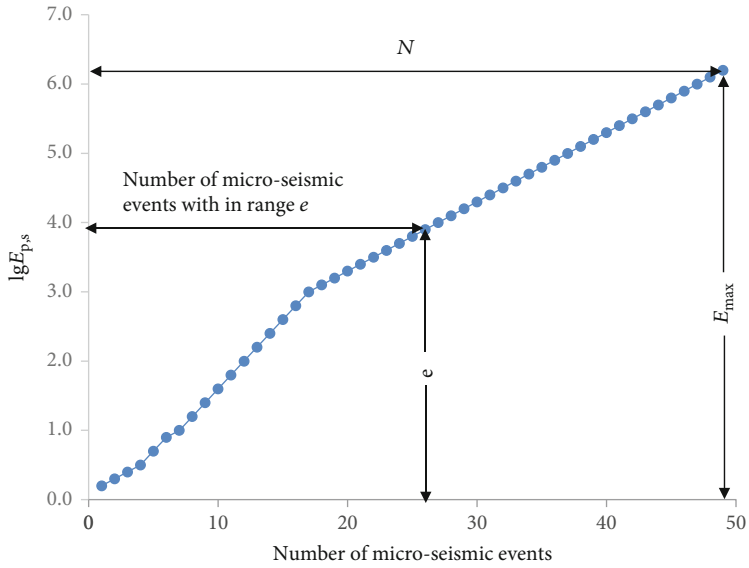

Figure 4: Energy released by microseismic events during the evolution of rock bursts (the microseismic events were arranged in chronological order; $E_{P,S}$ denotes the energy released from the microseismic events; E_{max} is the maximum microseismic energy; e denotes the energy range within E_{max}, and all microseismic events are arranged according to the magnitude of the energy thus released).

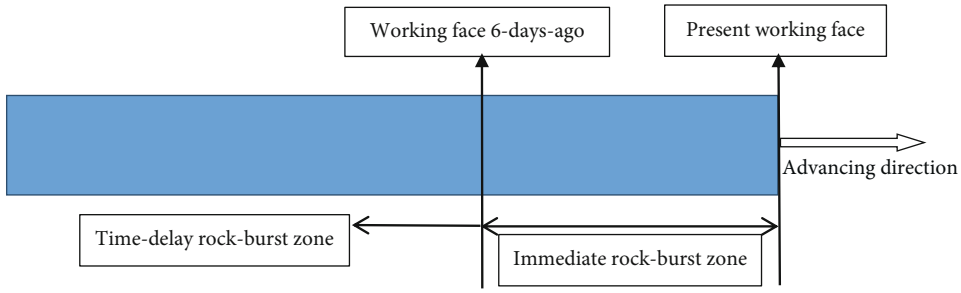

Figure 5: Classification criteria for immediate rock burst and time-delay rock burst.

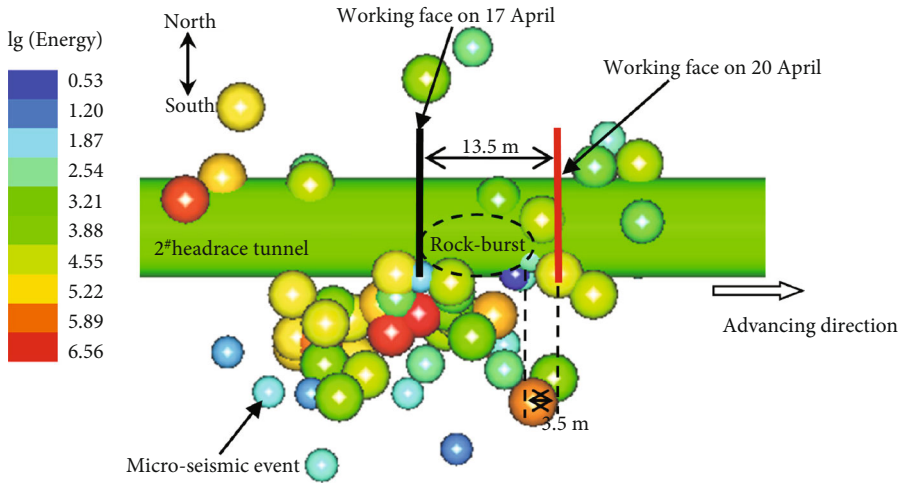

Figure 6: The spatial and energy distribution of microseismic events during the evolution of the rock burst on April 20, 2011 (note: there are ten-color scales in the figure, and the interval of log (energy) is 0.67 (from 0.53 to 6.56)).

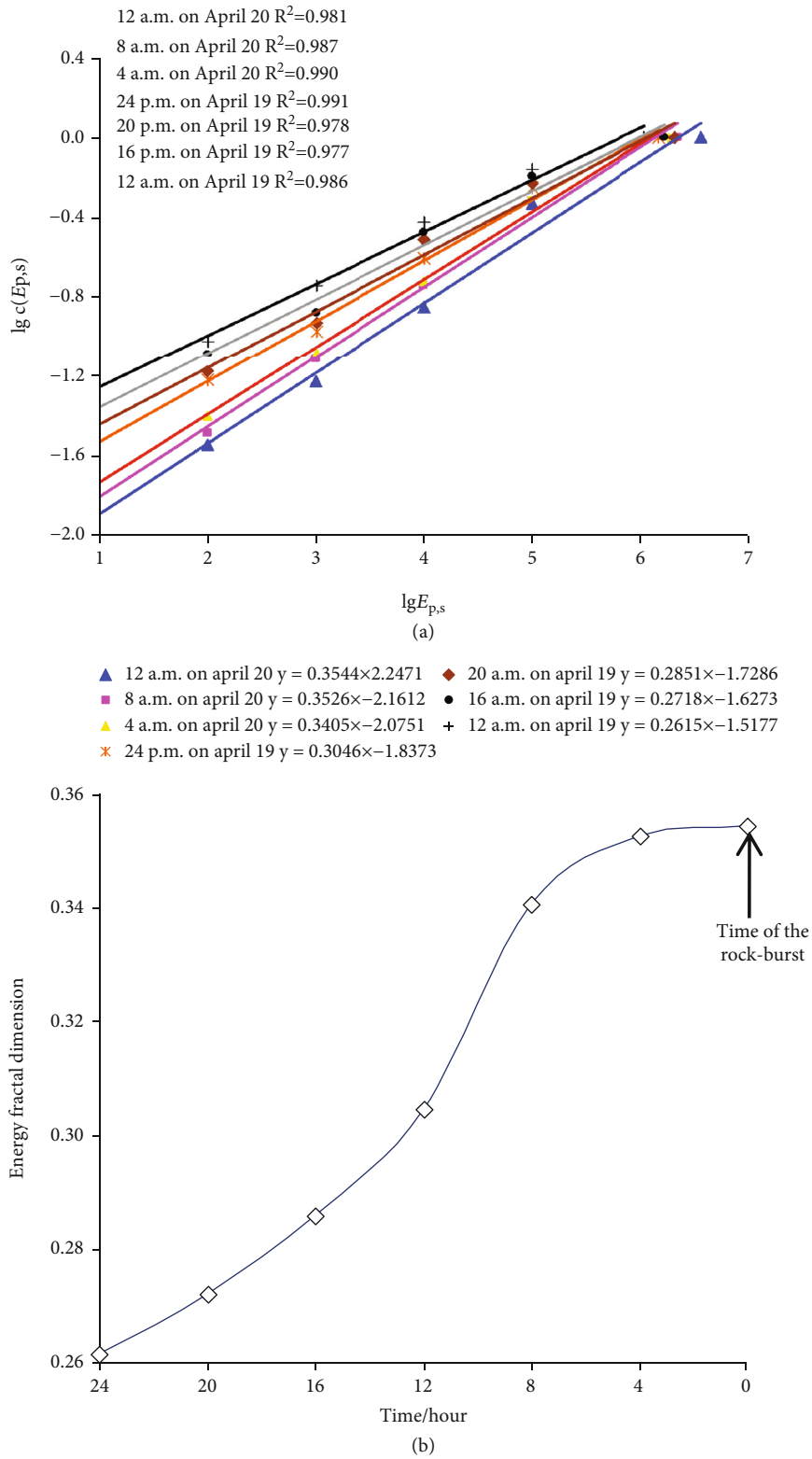

Figure 7: Energy fractal behavior within 24 hours for the rock burst on April 20, 2011. (a) Fitting chart of microseismic events. (b) Evolution of energy fractal dimension.

calculation in Figure 7 for microseismic events from 12:00 a.m. on April 18 to 12:00 a.m. on April 19, from 16:00 p.m. on April 18 to 16:00 p.m. on April 19, and from 12:00 a.m. on April 19 to 12:00 a.m. April 20, 2011. From Figure 7, we can see that there was a linear relationship between lg e and lg $c(e)$ (i.e., the self-similarity coefficient exceeded 0.986), which indicated that the energy distributions of microseismic events exhibited fractal behavior

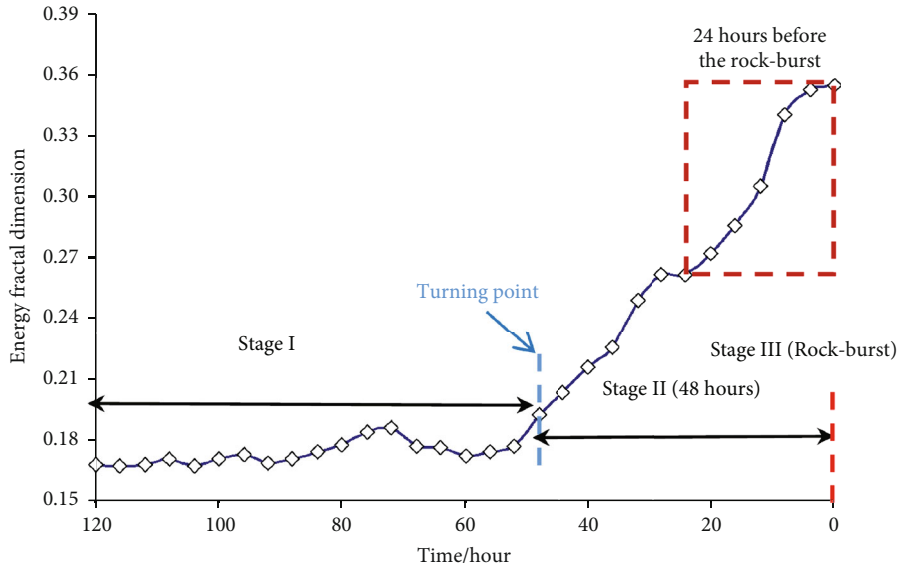

Figure 8: The energy fractal behavior of microseismic events associated with the evolution of the rock burst on April 20, 2011.

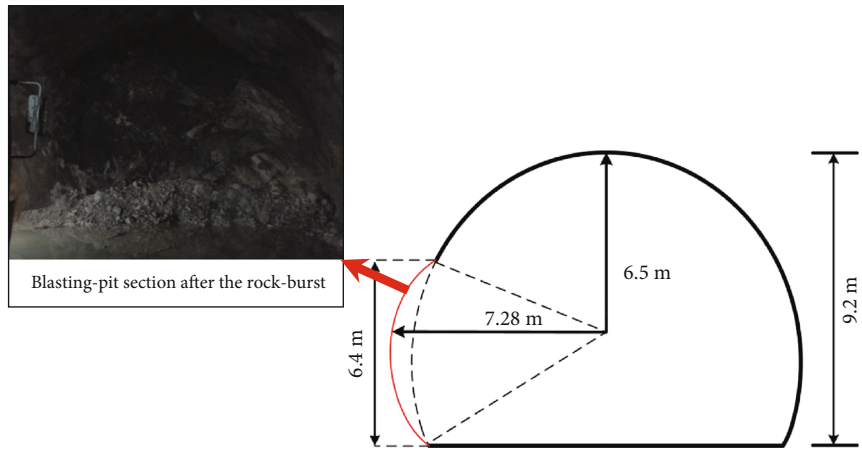

Figure 9: The immediate moderate rock burst on August 26, 2011.

and the energy fractal dimension of microseismic events increased as the rock burst approached.

Figure 8 demonstrates the evolution of energy fractal dimension associated with the rock burst on April 20, 2011. Figure 8 illustrates that the energy fractal dimension ranged from 0.16 to 0.36, which passed through the three stages necessary for the occurrence of a rock burst: Stage I (stabilization phase)—the energy fractal dimension of microseismic events in the rock burst zone was relatively stable at 0.16 to 0.20, at more than 48 h before the occurrence of the rock burst; Stage II (cumulative phase)—the energy fractal dimension increased from 0.20 to 0.36 as the rock burst approached, and the time range was within 48 h before the rock burst occurred; Stage III (rock burst phase)—when the energy fractal dimension reached its maximum value, the rock burst was imminent.

At 16:30 p.m. on August 26, 2011, when the working face had been excavated to chainage K8+294, there was a rock burst in the south wall from chainage K8+282 to K8+290, in the 3# headrace tunnel of Jinping-II hydropower station. The centerline of the rock burst pit was about 8.0 m behind the working face. The pit of the rock burst was approximately 0.9 m deep, 6.4 m high, and 9.0 to 8.5 m wide (as shown in Figure 9). The surrounding rock was thick with coarse grains and no surface plane therein. According to its time and area of occurrence, the rock burst on August 26, 2011 was defined as an immediate moderate rock burst. Using the energy fractal calculation method mentioned above, the energy fractal dimension of microseismic events during the evolution of the rock burst on August 26, 2011, is shown in Figure 10: the energy fractal dimension ranged from 0.17 to 0.28, which also increased as the rock burst developed on August 26, 2011, and passed through the usual three stages. The energy fractal dimension in Stage I (stabilization phase) ranged from 0.17 to 0.20; the energy fractal dimension in Stage II (cumulative phase) increased from 0.20 to 0.28 as the rock burst approached; the transition between Stages I and II occurred about 52 h before the rock

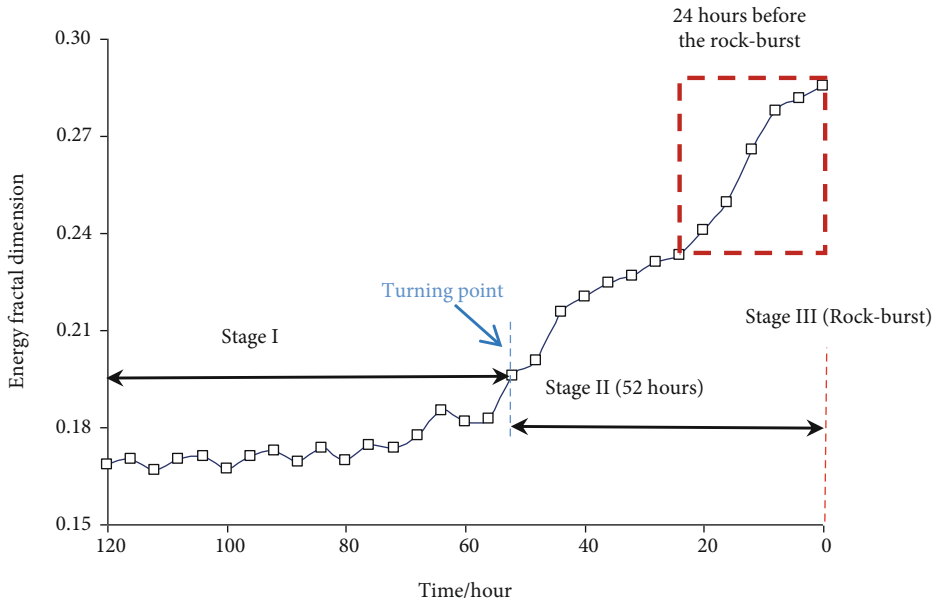

Figure 10: The energy fractal behavior of microseismic events associated with the evolution of the rock burst on August 26, 2011.

Table 2: Typical rock burst disasters.

No.	Rock burst intensity	Description of the rock burst	Photograph of the rock burst
1	Intense	Failure pit of the rock burst was approximately 1.2 m deep, 12 m wide, and 8.5 m high	
2	Moderate	Failure pit of the rock burst was approximately 0.78 m deep, 4.7 m wide, and 5 m high	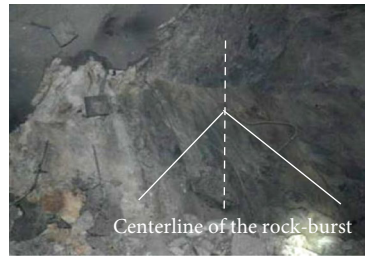

burst disaster. In Stage III (rock burst phase), when the energy fractal dimension reached its maximum value, the rock burst was imminent.

4.3. Quantitative Threshold of Energy Fractal Dimension for Immediate Rock Burst Warning. Microseismic events reflect the rupture of the surrounding rock. The distribution range and evolution of the energy fractal dimension of the microseismic events associated with the 37 rock burst disasters with different intensities were studied (typical rock burst disasters are summarized in Table 2). The results suggested that in the development of immediate rock bursts, the surrounding rock underwent three development stages of fracturing: in Stage I (stabilization phase), the energy fractal dimension of microseismic events in the rock burst zone was relatively stable, and below 0.2; in Stage II (cumulative phase), the energy fractal dimension of microseismic events in the rock burst zone increased constantly and approximated the maximum value just before the occurrence of the rock burst; in Stage III (rock burst phase), the energy fractal dimension reached its maximum value, accompanied by the occurrence of the rock burst disaster.

Stage II is of important reference significance for the prediction, warning, and control of rock burst disasters. The distribution of times to reach Stage II in the 37 rock bursts with different intensities is shown in Figure 11. As illustrated

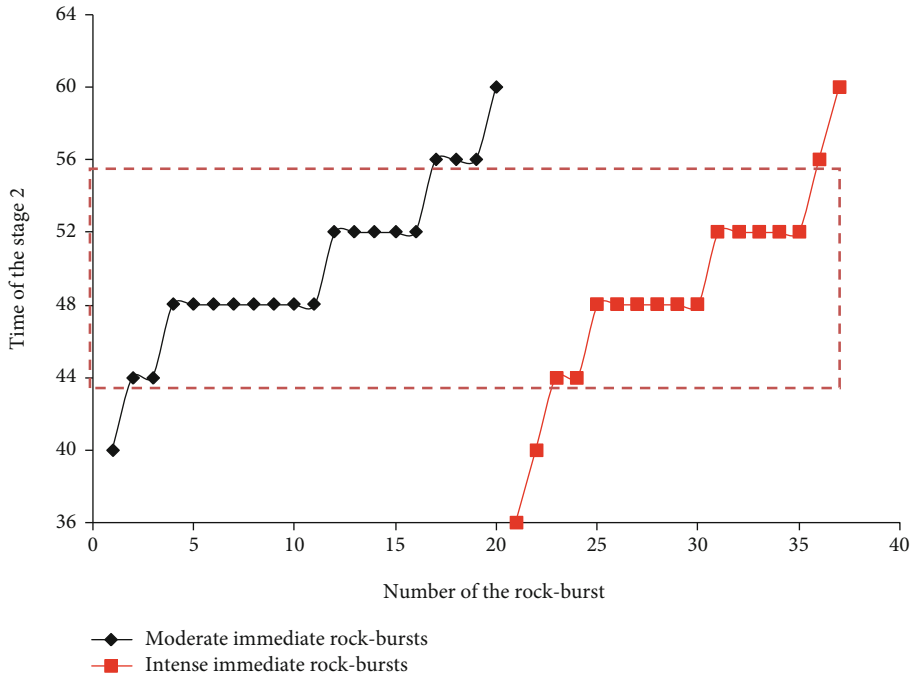

Figure 11: Distribution of durations of Stage II in the evolution of 37 immediate rock bursts of different intensities.

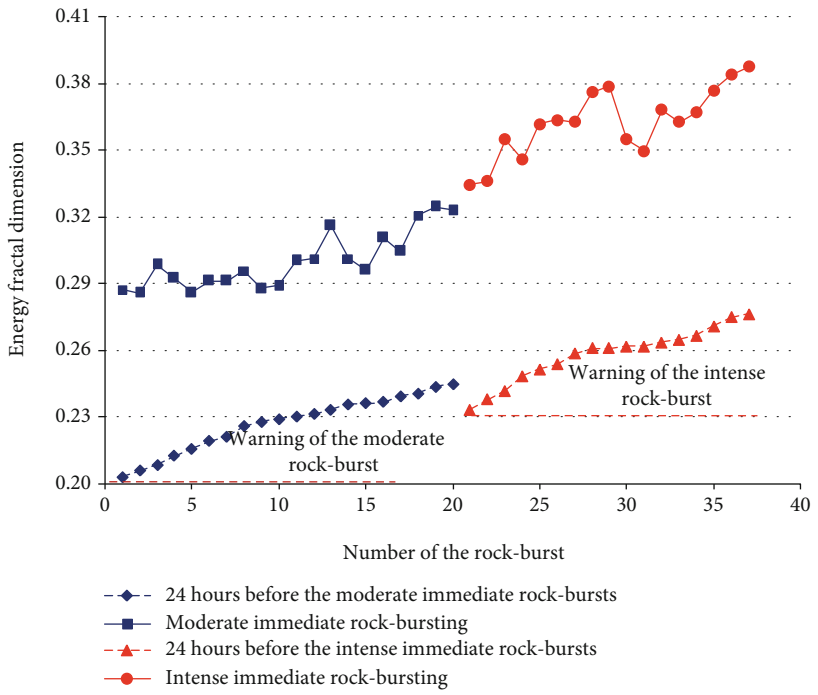

Figure 12: Comprehensive warning indices for different intensities of immediate rock burst (sorted by energy fractal dimension).

in the figure, the Stage II (cumulative phase) occurred from 36 to 64 h before a rock burst, therefore, to have enough time to guarantee that measures are taken to prevent rock burst disasters, the time range of 24 h before the occurrence of different intensities of rock burst disasters is taken as a warning index (this ensures that it covers the interval spanning Stage II and that there is enough time to guarantee that measures are taken timeously to prevent a rock burst disaster). The distribution of energy fractal dimensions in the 24 h before the occurrence of the 37 rock bursts of different intensities is depicted in Figure 12. A warning should be issued for a moderate immediate rock burst and an intense immediate rock burst when the energy fractal dimension exceeds 0.2 and 0.23, respectively.

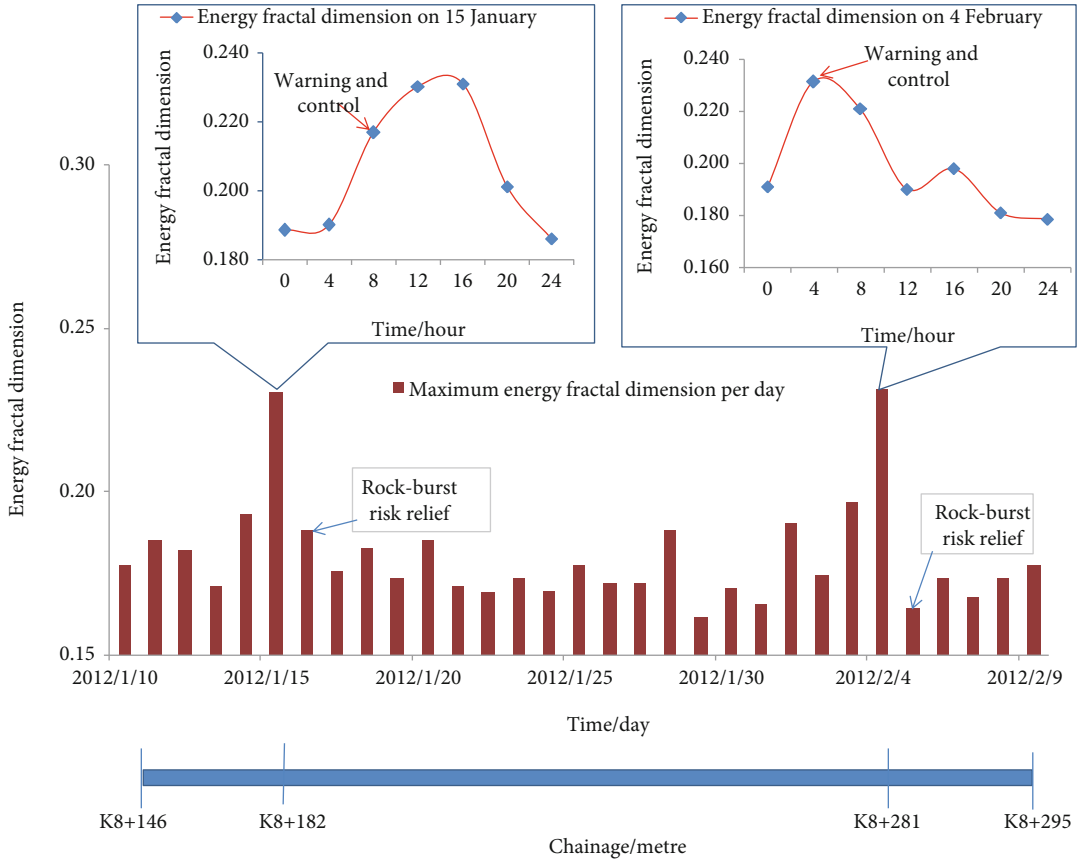

Figure 13: Evolution of maximum energy fractal dimensions for microseismic events occurring on each day during the excavation from January 15 to February 4, 2012 (chainages correspond to the excavation location for each day, unit: m).

4.4. Field Application of the Rock Burst Warning Index with Quantitative Threshold. The segment from chainage K9+146 to K9+295 of the 2# headrace tunnel in Jinping hydropower station was buried 2,342-2,509 m underground, which was under a maximum principal stress of 63 MPa, and UCS/σ_m = 1.75 [25]. Therefore, it is under the risk of intense rock bursts. By using the proposed method, a fractal calculation model was established to predict, warn, and dynamically control the potential rock burst risk during construction of the aforementioned segment. An example is given as follows: with the excavation of 2# headrace tunnel, the energy fractal dimensions of microseismic events on January 15, 2012 (working face reached chainage K8+182), and February 4, 2012 (working face reached chainage K8+281), both significantly increased. After issuing a warning of risk of these two rock bursts at 8 a.m. on January 15 and at 4 a.m. on February 4, 2012, when the energy fractal dimensions reached 0.2168 and 0.2312, respectively, the excavation was ceased to reduce disturbance. Meanwhile, prestressed hollow anchorage rods with a diameter and length of 30 mm and 6 m, respectively, were used. In this way, the bearing capacity of the surrounding rock mass was improved and the propagation of any cracks was controlled. Moreover, the support measures were taken close to the working face in the subsequent excavation process. After taking these measures, the energy fractal dimensions of microseismic events were decreased to 0.1757 (on January 16, 2012) and 0.1644 (on February 4, 2012), respectively. The energy fractal dimensions were both below the warning index threshold for an immediate rock burst, and the risk of a rock burst was alleviated (inhibition of potential rock bursts is shown in Figure 13).

5. Discussion

Energy fractal dimension is the measure of the regularity and order of energy distribution associated with microseismic events: the greater the proportion of large-energy microseismic events, the greater the microseismic energy fractal dimension. Therefore, during the evolution of immediate rock bursts, the energy fractal dimension of an intense rock burst was greater than that of a moderate rock burst, which was, in turn, larger than that without a rock burst, because the microseismic event energy distribution of the former was higher. Figure 14 illustrates the energy distribution of microseismic events in the zone of different intensities of immediate rock bursts (including intense rock bursts, moderate rock bursts, and no rock burst), which provide further evidence for the previous research (the risk and intensity of the immediate rock burst are increasing with the energy fractal dimension, and the energy fractal dimension can be

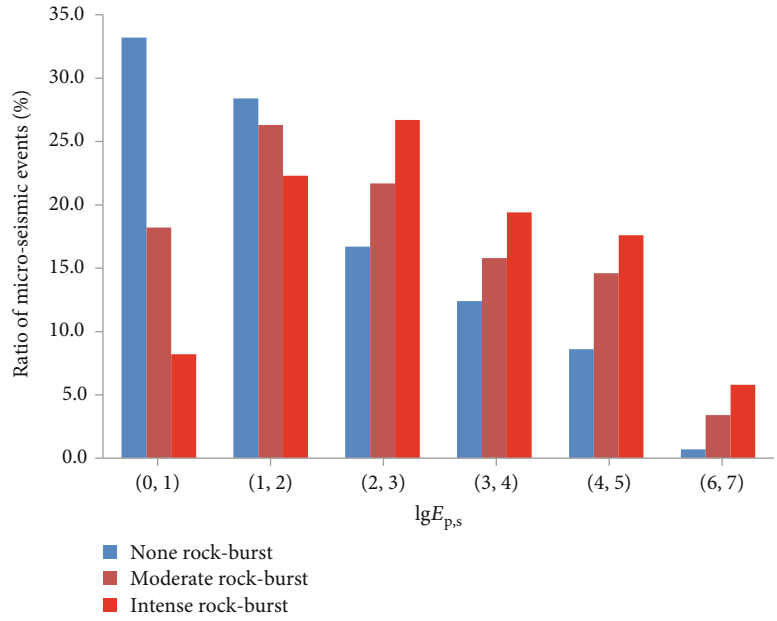

FIGURE 14: The ratio (percentage) distribution of microseismic energy for different intensities of immediate rock bursts (including intense rock bursts, moderate rock bursts, and no rock burst).

used as a dynamic warning index for different intensities of immediate rock bursts). At the same time, the dimensional accumulation of the microcrack distribution matched the rock failure process. The continuous accumulation thereof indicates that the surrounding rock mass is failing and when the energy fractal dimension increases to a certain value, a rock burst is imminent.

6. Conclusion

Based on different intensities of rock bursts occurring during construction of the deep tunnels at the Jinping hydropower station, the energy fractal behaviors of microseismic events in the development and occurrence of immediate rock bursts were investigated. A warning index based on energy fractal dimension with a quantitative threshold for immediate rock burst disaster warning in a deep tunnel was established.

The results show that the energy distribution of microseismic events during the evolution of immediate rock bursts (including moderate and intense rock bursts) demonstrates fractal properties. The fractal dimension of microseismic energy can be used as an index of energy release in deep tunnel excavation, which increases during the development of an immediate rock burst and reaches a maximum value as the rock burst occurs. For immediate rock bursts, if the intensity is lower, the energy fractal dimension thereof will be smaller. A warning should be issued for a moderate immediate rock burst and an intense immediate rock burst when the energy fractal dimension exceeds 0.2 and 0.23, respectively. Application shows that energy fractal dimension can be used as a dynamic warning index for immediate rock bursts of different intensities. Reasonable application of the above index can effectively reduce the potential risk of rock burst disasters in deep tunnel.

Data Availability

The data used to support the findings of this study are included within the article.

Conflicts of Interest

The authors declare no conflicts of interest.

Acknowledgments

The authors acknowledge the financial support from the National Natural Science Foundation of China (Nos. 42177156 and 51969007), the Fund of Jiangxi Provincial Department of Science and Technology (No. 20202ACBL214016), the Systematic Project of Guangxi Key Laboratory of Disaster Prevention and Engineering Safety (No. 2019ZDK034), and the Science and Technology Project of Jiangxi Provincial Department of Transportation (No. 2021Z0004). The original monitoring data were derived from State Key Laboratory of Geomechanics and Geotechnical Engineering Institute of Rock and Soil Mechanics, Chinese Academy of Sciences, Wuhan. The authors thank Professors Xia-ting Feng, Quan Jiang, Shao-jun Li, and Ya-xun Xiao for their support during micro-seismicity monitoring.

References

[1] N. G. W. Cook, E. Hoek, and J. P. G. Pretorius, "Rock mechanics applied to the study of rockbursts," *Journal of the South African Institute of Mining and Metallurgy*, vol. 66, no. 10, pp. 436–528, 1966.

[2] G. L. Feng, X. T. Feng, B. R. Chen, Y. X. Xiao, and Y. Yu, "A microseismic method for dynamic warning of rockburst

development processes in tunnels," *Rock Mechanics and Rock Engineering*, vol. 48, no. 5, pp. 2061–2076, 2015.

[3] M. Piotr and N. Zbigniew, "A comprehensive geomechanical method for the assessment of rockburst hazards in underground mining," *International Journal of Mining Science and Technology*, vol. 30, no. 3, pp. 345–355, 2020.

[4] J. Zhou, X. B. Li, and H. S. Mitri, "Evaluation method of rockburst: state-of-the-art literature review," *Tunnelling and Underground Space Technology*, vol. 81, pp. 632–659, 2018.

[5] G. L. Feng, X. T. Feng, Y. X. Xiao et al., "Characteristic microseismicity during the development process of intermittent rockburst in a deep railway tunnel," *International Journal of Rock Mechanics and Mining Sciences*, vol. 124, article 104135, 2019.

[6] A. Keneti and B. A. Sainsbury, "Review of published rockburst events and their contributing factors," *Engineering Geology*, vol. 246, pp. 361–373, 2018.

[7] C. Q. Zhang, X. T. Feng, H. Zhou, S. L. Qiu, and W. P. Wu, "A top pilot tunnel preconditioning method for the prevention of extremely intense rock-bursts in deep tunnels excavated by TBMs," *Rock Mechanics and Rock Engineering*, vol. 45, no. 3, pp. 289–309, 2012.

[8] X. T. Feng, H. S. Guo, C. X. Yang, and S. J. Li, "*In situ* observation and evaluation of zonal disintegration affected by existing fractures in deep hard rock tunneling," *Engineering Geology*, vol. 242, pp. 1–11, 2018.

[9] C. Q. Zhang, X. T. Feng, H. Zhou, S. L. Qiu, and W. P. Wu, "Case histories of four extremely intense rockbursts in deep tunnels," *Rock Mechanics and Rock Engineering*, vol. 45, no. 3, pp. 275–288, 2012.

[10] B. Li, N. W. Xu, F. Dai, G. K. Gu, and W. Ke, "Microseismic monitoring and stability analysis for the large-scale underground caverns at the Wudongde hydropower station," *Bulletin of Engineering Geology and the Environment*, vol. 79, no. 7, pp. 3559–3573, 2020.

[11] B. Li, N. W. Xu, F. Dai, G. L. Zhang, and P. W. Xiao, "Dynamic analysis of rock mass deformation in large underground caverns considering microseismic data," *International Journal of Rock Mechanics and Mining Sciences*, vol. 122, article 104078, 2019.

[12] J. S. Zhao, X. T. Feng, Q. Jiang, and Y. Y. Zhou, "Microseismicity monitoring and failure mechanism analysis of rock masses with weak interlayer zone in underground intersecting chambers: a case study from the Baihetan Hydropower Station, China," *Engineering Geology*, vol. 245, pp. 44–60, 2018.

[13] R. J. Durrheim, A. Haile, M. K. C. Roberts, J. K. Schweitzer, S. M. Spottiswoode, and J. W. Klokow, "Violent failure of a remnant in a deep South African gold mine," *Tectonophysics*, vol. 289, no. 1-3, pp. 105–116, 1998.

[14] L. Z. Tang and K. W. Xia, "Seismological method for prediction of areal rockbursts in deep mine with seismic source mechanism and unstable failure theory," *Journal of Central South University of Technology*, vol. 17, pp. 947–953, 2010.

[15] G. L. Feng, B. R. Chen, Y. X. Xiao et al., "Microseismic characteristics of rockburst development in deep TBM tunnels with alternating soft–hard strata and application to rockburst warning: A case study of the Neelum–Jhelum hydropower project," *Tunnelling and Underground Space Technology*, vol. 122, article 104398, 2022.

[16] Y. Yu, B. T. Zhu, H. S. Guo, B. R. Chen, and D. X. Geng, "Warning index associated with rock burst in deeply buried tunnels," *International Journal of Geomechanics*, vol. 21, no. 11, article 04021211, 2021.

[17] B. B. Mandelbrot, D. E. Passoja, and A. J. Paullay, "Fractal character of fracture surfaces of metals," *Nature*, vol. 308, pp. 721-722, 1984.

[18] H. P. Xie and W. G. Pariseau, "Fractal character and mechanism of rock bursts," *International Journal of Rock Mechanics and Mining Sciences & Geomechanics Abstracts*, vol. 30, no. 4, pp. 343–350, 1993.

[19] X. T. Feng, Y. Yu, G. L. Feng, Y. X. Xiao, B. R. Chen, and Q. Jiang, "Fractal behaviour of the micro-seismic energy associated with immediate rockbursts in deep, hard rock tunnels," *Tunnelling and Underground Space Technology*, vol. 58, pp. 98–107, 2016.

[20] D. J. L. Alexander and P. P. John, "The deep structure and rheology of a plate boundary-scale shear zone: constraints from an exhumed Caledonian shear zone, NW Scotland," *Lithosphere*, vol. 2021, article 8824736, 2021.

[21] M. Debjeet and P. N. S. Roy, "Fractal and seismic *b*-value study during dynamic roof displacements (roof fall and surface blasting) for enhancing safety in the longwall coal mines," *Engineering Geology*, vol. 253, pp. 184–204, 2019.

[22] Y. Bai, S. Q. Liu, Z. H. Xia, Y. X. Chen, G. Y. Liang, and Y. Shen, "Fracture initiation mechanisms of multibranched radial-drilling fracturing," *Lithosphere*, vol. 2021, article 3316083, 2021.

[23] W. L. Lin, A. Liu, W. W. Mao, Z. Maqsood, and K. Junichi, "Micromechanical behavior of granular soils characterized by acoustic emission," *Lithosphere*, vol. 2021, article 4061808, 2021.

[24] Y. Lu, S. H. Liu, L. P. Weng, L. J. Wang, Z. Li, and L. Xu, "Fractal analysis of cracking in a clayey soil under freeze-thaw cycles," *Engineering Geology*, vol. 208, pp. 93–99, 2016.

[25] B. R. Chen, X. T. Feng, Q. P. Li, R. Z. Luo, and S. J. Li, "Rock burst intensity classification based on the radiated energy with damage intensity at Jinping II hydropower Station, China," *Rock Mechanics and Rock Engineering*, vol. 48, no. 1, pp. 289–303, 2015.

[26] A. J. Mendecki, *Seismic Monitoring in Mines*, Chapman & Hall, London, 1997.

[27] B. B. Mandelbrot, *The Fractal Geometry of Nature*, W. H. Freeman and Company, 1982.